Chemical Science

ROYAL SOCIETY OF CHEMISTRY

EDGE ARTICLE

View Article Online
View Journal | View Issue

Cite this: *Chem. Sci.*, 2025, **16**, 6089

All publication charges for this article have been paid for by the Royal Society of Chemistry

Cysteine-selective [^{188}Re]Re(v) radiolabelling of a Nanobody® for targeted radionuclide therapy using a "chelate-then-click" approach†

Diana R. Melis, [ab] Charlotte Segers, [a] Jasmien Wellens, [a] Michiel Van de Voorde, [a] Olivier Blacque, [c] Maarten Ooms, [a] Gilles Gasser *[b] and Tomas Opsomer *[a]

Received 14th November 2024
Accepted 25th February 2025

DOI: 10.1039/d4sc07743a

rsc.li/chemical-science

In this study, we present the first reported use of bioorthogonal click chemistry with rhenium-188 for radiolabelling of an anti-c-Met V_HH Nanobody®. We employed a "chelate-then-click" strategy, wherein a bifunctional chelator was designed in two parts, which were subsequently joined post-labelling and post-conjugation *via* the strain-promoted azide–alkyne cycloaddition (SPAAC) reaction. Cysteine-selective conjugation of the V_HH was achieved through thiol-Michael addition, forming a V_HH-DBCO construct. Radiolabelling of the azide-functionalised chelator with [^{188}Re]Re(v) was optimised to achieve a radiochemical conversion of ~70%, despite challenges associated with maintaining the azide functionality under reducing conditions. The final product, [^{188}Re]Re-V_HH, demonstrated high radiochemical purity and good *in vitro* stability over 48 h. *In vitro* cell-binding studies against U87MG and BxPC3 cell lines proved the retention of c-Met binding post-labelling. *In vivo* biodistribution studies on mice bearing BxPC3 tumour xenografts, however, exhibited suboptimal tumour uptake, likely a result of the low molar activity (1.4–3.3 MBq nmol^{-1}) of the radioconjugate. This work illustrates the potential of bioorthogonal click chemistry for radiolabelling biomolecules with ^{188}Re, although further optimisation or alternative radiolabelling strategies to enhance the molar activity are necessary to improve pharmacokinetics.

1. Introduction

Rhenium-188, with its favourable physical properties and generator production, has often been recognised as an attractive radionuclide in the targeted treatment of cancer. In addition to its emission of high-energy β^- particles (E_{max} = 2.12 MeV, E_{av} = 763 keV) and relatively short 16.9 h half-life, ^{188}Re is readily available as no-carrier-added perrhenate ([^{188}Re]ReO_4^-) from a ^{188}W/^{188}Re generator.[1–3] The latter makes the development of ^{188}Re-radiopharmaceuticals of particular interest, as generator-based radionuclides can be eluted on demand at reasonable costs and with high specific activity. ^{188}Re is the group 7 congener of the widely used SPECT imaging radionuclide, ^{99m}Tc, sharing many chemical similarities and, therefore, chelator systems as well.[4] Since the ability to reduce [^{188}Re]ReO_4^- and prevent its reoxidation to the +7 oxidation state is more difficult than for [^{99m}Tc]TcO_4^-, harsher labelling conditions for ^{188}Re than used with ^{99m}Tc (higher temperatures, more reducing agent, *etc.*) are often required.[5,6] Additionally, effort needs to be put towards finding a chelator system that ensures a high level of chemical inertness and stability for ^{188}Re, particularly *in vivo*. The tetradentate N_xS_{4-x} chelator system has been used extensively to coordinate Tc(v) and Re(v) to form well-defined, stable complexes.[1,7,8] In particular, N_2S_2 monoamine-monoamide dithiol (MAMA) chelators are especially attractive, as MAMA derivatives complexed with ^{99m}Tc(v) and $^{186/188}$Re(v) are neutral and have been shown to be stable under physiological conditions.[9–13] Additionally, the single amine on N_2S_2 MAMA chelators, as opposed to the two amines on N_2S_2 bis(aminoethanethiol) (BAT) chelators or no amines on N_2S_2 diamido-dithiol (DADS) chelators (Fig. 1), allows for the easy and unambiguous conjugation of a targeting vector such as a small molecule, peptide or biomolecule.[13]

While antibodies are the biomolecules most frequently used as targeting vectors in targeted radionuclide therapy (TRNT), the 16.9 h half-life of ^{188}Re makes it more compatible with vectors that have shorter biological half-lives.[14] There has been

[a]*Nuclear Medical Applications (NMA), Belgian Nuclear Research Centre (SCK CEN), Mol 2400, Belgium. E-mail: tomas.opsomer@sckcen.be*

[b]*Chimie ParisTech, PSL University, CNRS, Institute of Chemistry for Life and Health Sciences, Paris 75005, France. E-mail: gilles.gasser@chimieparistech.psl.eu; Web: https://www.gassergroup.com*

[c]*Department of Chemistry, University of Zurich, Winterthurerstrasse 190, Zurich 8057, Switzerland*

† Electronic supplementary information (ESI) available: Full experimental, characterisation and X-ray crystallographic details. Crystallographic data for **Re-2** and **Re-3**. CCDC [2384422 and 2384423]. For ESI and crystallographic data in CIF or other electronic format see DOI: https://doi.org/10.1039/d4sc07743a.

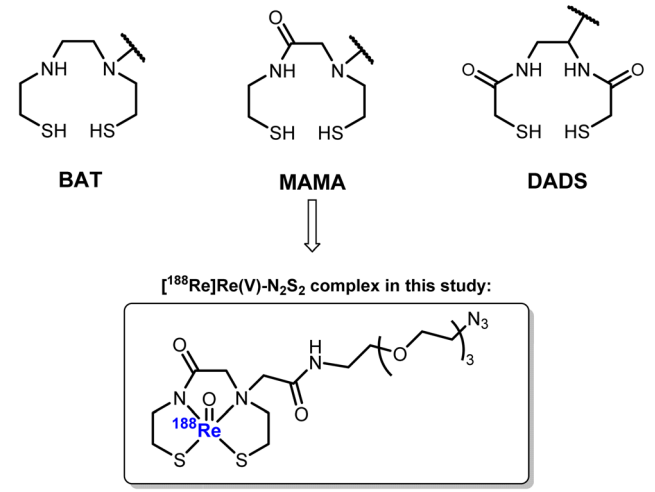

Fig. 1 Examples of N_2S_2 chelators for chelating ^{99m}Tc(v) and $^{186/188}$Re(v), and the [^{188}Re]Re(v)-N_2S_2 complex used in this study.

a growing interest in the use of Nanobodies® (V_HH, variable domain of the heavy chain of heavy-chain only antibodies) as they have several favourable advantages, particularly when it comes to their *in vivo* pharmacokinetics.[14–16] They are among the smallest known antigen-binding antibody fragments (~15 kDa), which gives them excellent tumour penetration properties, as well as the ability to pass through the glomerular filtration barrier for rapid excretion.[15,16] Their small size, however, often does not allow for sufficient residence time in the bloodstream, which is a requirement for adequate tumour accumulation.[17] For this reason, the plasma half-life of a V_HH is oftentimes increased by the addition of a biological half-life extending (HLE) group, such as one which binds to serum albumin,[17,18] or tuned by PEGylation.[19] This helps to provide a balance between excretion and unwanted radiation toxicity side-effects for successful therapy.

Herein, we describe the radiolabelling of a HLE anti-c-Met V_HH with [^{188}Re]Re(v)-N_2S_2 (Fig. 1). C-Met is a membrane receptor protein belonging to the receptor tyrosine kinase family and is commonly activated by hepatocyte growth factor.[20] Once activated, it stimulates cell proliferation and motility, including the invasion and migration of cancer cells, making it a good target in the treatment of cancer.[20] However, the radiolabelling of a heat-sensitive biomolecule, such as a V_HH, with ^{188}Re(v) involves several challenges. The harsh labelling conditions of the Re(v)-oxo core would effectively destroy any sensitive biomolecule in the process. Additionally, it is preferred to attach bifunctional chelators to biomolecules in a site-specific manner in order to produce well-defined conjugates with retained affinity.[21] Since this usually involves a cysteine-mediated conjugation and the chelator of choice, N_2S_2, contains free thiols prior to radiolabelling, it seemed almost impossible to proceed with this method. Post-conjugation labelling would destroy the V_HH, while pre-conjugation labelling would result in the free thiols of the bifunctional chelator reacting with the Michael-acceptor needed for bioconjugation. For this reason, we turned to the efficient method of bioorthogonal click chemistry. With the advent of bioorthogonal click chemistry, more possibilities than ever before are available in the fields of radioimaging and radiotherapy.[22] In particular, the copper-free strain-promoted azide–alkyne cycloaddition (SPAAC) and inverse electron demand Diels–Alder (IEDDA) reactions have shown promise in the development of radiopharmaceuticals because of their mild reaction conditions and

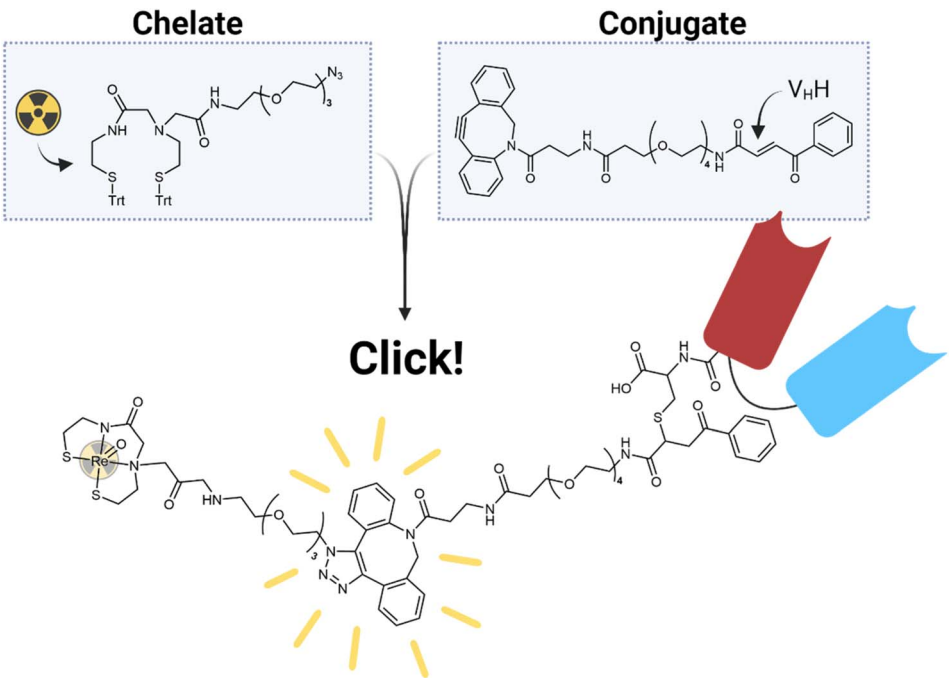

Fig. 2 The "chelate-then-click" labelling strategy employed in this study.

relatively quick reaction times.[23] In this work, we employed SPAAC in a "chelate-then-click" approach to effectively radiolabel a V_HH with ^{188}Re (Fig. 2). This method found success with Lodhi *et al.* in the labelling of human serum albumin with ^{99m}Tc.[24] To our knowledge, this is the first reported use of bioorthogonal click chemistry with ^{188}Re.

2. Results and discussion

2.1 Synthesis

The N_2S_2 MAMA ligand was chosen as a suitable chelator as it is known to form a stable neutral complex with Re(v), the most easily accessible oxidation state of Re from perrhenate.[25] Additionally, to our knowledge, this chelator has not yet been investigated for the labelling of a heat-sensitive biomolecule such as a V_HH with ^{188}Re. The trityl-protected N_2S_2 MAMA chelator (**1**) was synthesised in two steps according to a literature procedure.[10] Reaction of the chelator with ethyl bromoacetate and subsequent saponification of the ester (**2**) yielded the chelator with a pendant carboxylic acid (**3**), as described previously.[26] This acid allowed for the amide coupling of H_2N-PEG_3-N_3 to produce N_2S_2-PEG_3-N_3 (**4**) (Scheme 1A). The dibenzocyclooctyne (DBCO)-functionalised carbonylacrylic (CA) compound for cysteine V_HH modification was synthesised *via* a series of amide couplings, resulting in DBCO-PEG_4-CA (**7**) (Scheme 1C). Detailed spectra and characterisation data are provided in the ESI.†

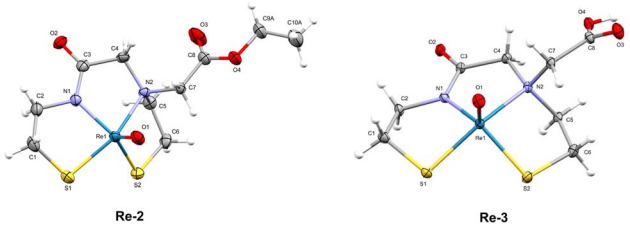

Fig. 3 ORTEP diagrams of the crystal structures of **Re-2** and **Re-3** (thermal ellipsoids are drawn at the 30% probability level for both).

The "cold" ^{nat}ReO(N_2S_2-PEG_3-N_3) complex (**Re-4**) was synthesised in three steps, starting with the deprotection of the *S*-trityl groups on ester compound **2** with TFA and triethylsilane (Scheme 1B). The deprotected chelator **2** was then reacted with $(Ph_3P)_2ReOCl_3$ in the presence of NaOAc to form complex **Re-2**. Subsequent saponification of the ester yielded **Re-3** and amide coupling with H_2N-PEG_3-N_3 thereafter produced the ^{nat}ReO(N_2S_2-PEG_3-N_3) complex, **Re-4** (Scheme 1B). The synthesis of **Re-4** had to be performed over three steps to prevent the Staudinger reduction of the azide by the PPh_3 ligands of the $(Ph_3P)_2ReOCl_3$ precursor. The ^{1}H NMR spectra of all three rhenium complexes exhibit complex splitting patterns as a result of the chelator backbone protons becoming diastereotopic upon coordination to the Re(v) oxo core. Additionally, all chemical shifts of the chelator protons on **Re-4** are present

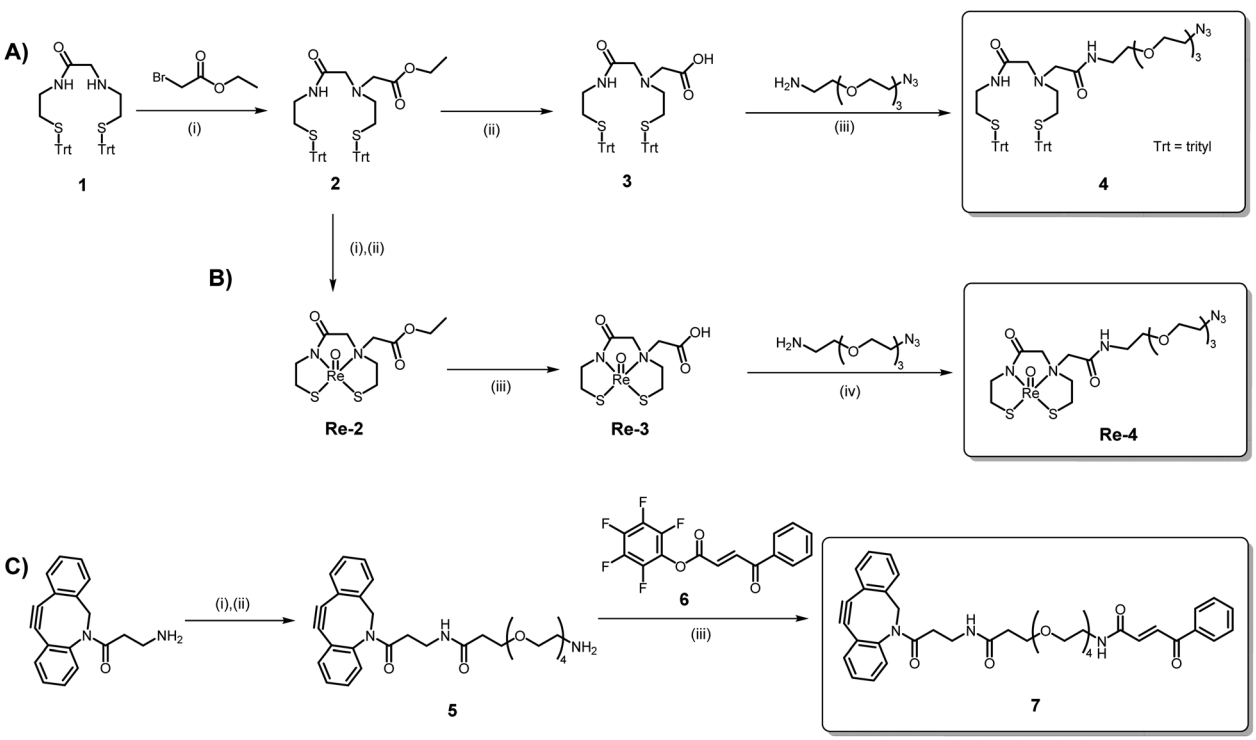

Scheme 1 (A) Synthesis of the N_2S_2-PEG_3-N_3 chelator, **4**. Reagents and conditions: (i) DIPEA, MeCN, 85 °C, 4 h (84%); (ii) LiOH, THF/H_2O, r.t., 20 h (91%); (iii) EDC, HOBt, DCM, r.t., 20 h (58%). (B) Synthesis of the ^{nat}ReO(N_2S_2-PEG_3-N_3) complex, **Re-4**. Reagents and conditions: (i) TFA, Et_3SiH, 0 °C, 20 min. (ii) $(PPh_3)_2ReOCl_3$, NaOAc, MeOH, 75 °C, 18 h (62%); (iii) LiOH, THF/H_2O, r.t., 2 h (68%); (iv) EDC, HOBt, DMF, r.t., 20 h (30%). (C) Synthesis of the DBCO-PEG_4-CA ligand, **7**. Reagents and conditions: (i) Boc-NH-PEG_4-COOH, DIPEA, DCM, r.t., 20 h; (ii) TFA, DCM, r.t., 1 h (81%); (iii) DCM, DIPEA, r.t., 20 h (80%).

downfield upon complexation compared to the trityl-protected ligand, **4**, with the exception of the protons on the carbon alpha to the amine (protons e, Fig. S17†). These protons experience a dramatic splitting where one proton shifts upfield (1.57 ppm) and one shifts downfield (3.95 ppm). This is indicative of the *syn* isomer of the complex being formed, as previously observed.[13,26] The *syn* configuration of the isolated Re complexes was confirmed by the X-ray crystal structures obtained for **Re-2** and **Re-3** (Fig. 3).

2.2 X-ray crystallography

Crystals of **Re-2** and **Re-3** were analysed by X-ray diffraction (Fig. 3). The crystal data for both complexes are summarised in Table S1.† Both complexes have a distorted square-pyramidal geometry as described previously for similar N_2S_2 complexes.[27–30] The complexes are "distorted" in the way that the rhenium(v) oxo group lies above the plane of the four basal nitrogen and sulphur atoms. Both structures have the pendant ester (**Re-2**) or carboxylic acid (**Re-3**) functionality on the same side as the apical Re=O group, confirming the *syn* isomer was formed. Additionally, each of the crystals for **Re-2** and **Re-3** contain both enantiomers of the *syn* conformation in a 1 : 1 ratio.

2.3 Cysteine-selective V_HH bioconjugation

The bivalent HLE anti-c-Met V_HH provided by Sanofi® was engineered at its C-terminus with a terminal cysteine residue, allowing for cysteine-selective V_HH bioconjugation. A carbonylacrylic (CA) moiety was chosen as the Michael-acceptor for this conjugation as it has been shown to be highly selective for cysteines in stoichiometric quantities, rapidly forming a stable product under biocompatible conditions.[31,32] Most importantly, unlike with maleimides which have shown instability *in vivo*,[33] the thioether product formed by addition of a cysteine onto a CA moiety has been reported to be irreversible.[31,32]

Since the free thiols of the V_HH constructs are cross-reactive with each other, dimerisation happens readily in basic or neutral solutions. To free the thiol for bioconjugation, the V_HH dimer (V_HH-S–S-V_HH) was cleaved using dithiothreitol (DTT) at room temperature to yield the monomer (V_HH-SH). This reaction was monitored *via* size exclusion high performance liquid chromatography (SEC-HPLC), which showed only one peak corresponding to the monomer after 1 h (Fig. S24†). Removal of the excess DTT using a PD-10 desalting column and immediate reaction with 3 equivalents of DBCO-PEG_4-CA (**7**) for 1.5 h yielded the desired DBCO-PEG_4-V_HH construct (Fig. 4). ESI-MS analysis of the conjugate after a final PD-10 purification showed a single mass after deconvolution corresponding to the expected mass of the desired V_HH-DBCO construct (Fig. S26B†). The total protein recovery of the bioconjugation was 71 ± 3% and the purity of the conjugate was determined to be ~97% by SEC-HPLC (Fig. S27†).

2.4 ^{188}Re(v)-radiolabelling of N_2S_2-PEG_3-N_3 (4)

No-carrier-added [^{188}Re]ReO_4^- was eluted from an in-house built ^{188}W/^{188}Re generator using saline. The perrhenate was

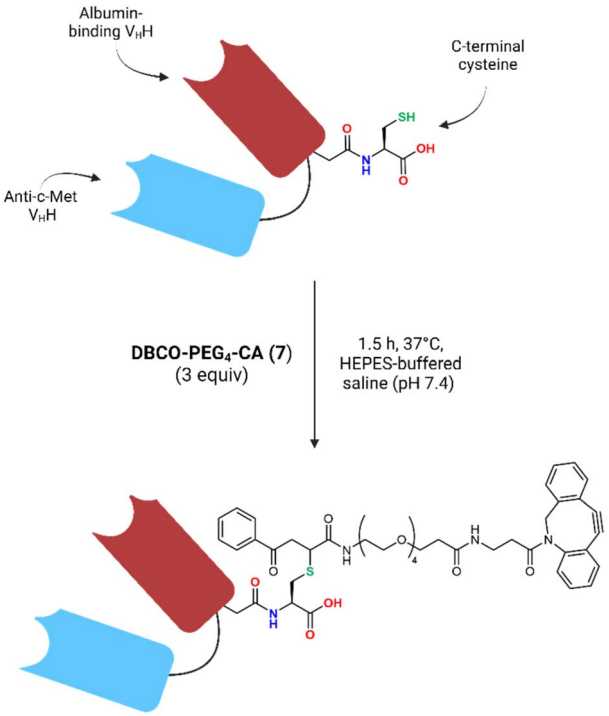

Fig. 4 Schematic overview of the conjugation of the V_HH with DBCO-PEG_4-CA (**7**).

concentrated after elution to provide a sufficient activity concentration for radiolabelling (~500 MBq mL^{-1}). A report on the construction of the generator and quality control of its eluate is referenced in the ESI.† To monitor the reaction process and optimise the radiolabelling effectively, [^{188}Re]ReO(N_2S_2-PEG_3-N_3) was synthesised in two steps (Scheme S1†). The aim was first to produce a [^{188}Re]Re(v)-citrate precursor by reducing [^{188}Re]ReO_4^- in citrate buffer in the presence of the reducing agent, stannous chloride ($SnCl_2$),[34,35] and then add an aliquot of this to the freshly-deprotected N_2S_2 chelator (**4**) to afford the final labelled compound, [^{188}Re]ReO(N_2S_2-PEG_3-N_3), after transchelation. Ascorbic acid was also included in both steps as an antioxidant to keep the ^{188}Re-labelled compounds stable. Initial radiolabelling attempts with the N_2S_2-PEG_3-N_3 chelator (**4**), however, yielded three distinct peaks on the radio-HPLC chromatogram (Fig. 5). Upon further investigation and comparison to the HPLC-UV chromatogram of the ^{nat}Re(v) analogue, **Re-4**, it was determined that the minor peak (retention time 7.4 min) in the radiochromatogram corresponds to the labelled chelator with the azide group intact. The two largest peaks (retention times 6.4 and 6.6 min), however, were attributed to reduction products resulting from an excess of $SnCl_2$ in the labelling mixture. This was proven by treating **Re-4** with $SnCl_2$, which led to the formation of two additional distinct Re(v) complexes according to ESI-MS (Fig. S31 and S32†). HPLC analysis demonstrated that these products co-elute with the byproducts observed in the labelling mixture (Fig. 5 and S33–S35†). Increasing the amount of $SnCl_2$ resulted in the exclusive formation of the product corresponding to the peak at 6.4 min (Fig. 5), and ESI-MS data enabled the assignment of this peak to

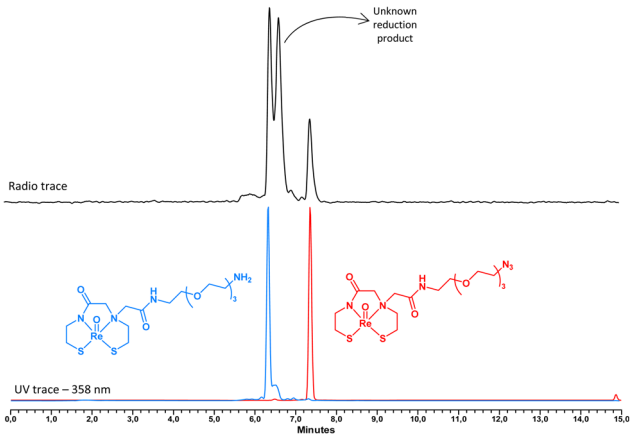

Fig. 5 Radio-HPLC chromatogram of the crude labelling mixture (black) compared to the UV chromatograms of the ^{nat}Re(v) complexes, **Re-4** (red) and ^{nat}ReO(N_2S_2-PEG_3-NH_2), produced by the reduction of **Re-4** by excess $SnCl_2$ in ethanol at room temperature (blue).

the amine derivative formed *via* reduction of the azide. Further evaluation of the reduction of **Re-4** under radiolabelling conditions at varying pH values (4, 5, and 5.7) indicated that the formation of the amine is slightly favoured at lower pH (Fig. S33–S35†). The identity of the middle peak ($m/z = 628.3$) at retention time 6.6 min remains undetermined, however, the available evidence strongly suggests that it represents another Re complex and a reduction product.

Unfortunately, having the azide reduced would prevent the SPAAC click reaction from taking place with the DBCO-PEG_4-V_HH construct in the subsequent step. Switching the click reagents (*i.e.* the DBCO and N_3) between the two halves would also not work as the DBCO is unstable in the presence of the excess TFA required to remove the protecting groups of the chelator.[36] Having the azide on the half with the CA is additionally unfavourable as azides have been reported to react with α,β-unsaturated carbonyl compounds.[37] It was therefore decided to keep the azide on the chelator and optimise the radiolabelling. Careful optimisation of the radiolabelling conditions to maximise the ratio of azide to amine and perrhenate were performed, testing factors such as $SnCl_2$ concentration (0.0–1.5 μg μL^{-1}), chelator amount (0.01–0.5 μmol), reaction volume (0.1–1.0 mL), temperature (40 °C or 90 °C) and reaction time (15–60 min), as well as the influence of having a N_2 atmosphere. The results of these optimisations are displayed in Fig. 6. The ultimate goal was to decrease the amount of $SnCl_2$ to a concentration low enough to prevent azide reduction but high enough to reduce Re(VII) to Re(V).

$SnCl_2$ concentration and influence of N_2. It is known that in comparison to Tc(VII), a large excess of Sn(II) is usually required to sufficiently reduce Re(VII) to its lower oxidation states. This is as a result of the lower standard reduction potential of Re(VII) over Tc(VII).[38] Performing the reduction in an acidic citrate solution significantly increases the ease of reduction of [^{188}Re]ReO_4^- by an effect known as the "expansion of the coordination sphere," leading to an increase in the standard reduction potential and thus a decrease in the concentration of Sn(II) required.[39,40]

Initially, our radiolabelling experiments were conducted in the presence of air with no N_2 purging of the citrate buffer. These experiments showed that over 1.0 μg μL^{-1} of $SnCl_2$ was necessary to achieve a radiochemical conversion (RCC) to [^{188}Re]Re(V)-citrate greater than 95% (Fig. 6A, pink curve). However, when the resultant [^{188}Re]Re(V)-citrate was reacted with the N_2S_2-PEG_3-N_3 chelator (**4**) in the presence of air, the RCC to [^{188}Re]ReO(N_2S_2-PEG_3-N_3) was only about 50% (Fig. 6B, pink curve). This prompted further optimisation of the radiolabelling conditions to improve the yield. Subsequent experiments were performed in a N_2 atmosphere using N_2-purged citrate buffer while varying the concentration of $SnCl_2$ (0.025–1.50 μg μL^{-1}). The activity (20 MBq), volume (100 μL), chelator quantity (0.1 μmol), temperature (90 °C) and time (60 min) were kept constant. The results indicate that under a N_2 atmosphere, the required $SnCl_2$ concentration could be reduced by ten times (0.1 μg μL^{-1}) to achieve a RCC greater than 95%, compared to the reaction in the presence of air (Fig. 6A). In fact, to our knowledge, we were able to reach a concentration of $SnCl_2$ per MBq of activity lower than any recorded concentration in literature for the reduction of ^{188}Re(VII) to ^{188}Re(V). This was oftentimes 15 to 20 times lower (and sometimes up to 200 times lower) than published values,[34,41–45] bringing it closer to the concentration range of $SnCl_2$ used for the reduction of [^{99m}Tc]TcO_4^-. This was an important outcome for the labelling of our chelator bearing a reducible azide. Fig. 6B shows that by maintaining a constant chelator concentration and adjusting the $SnCl_2$ concentration, the maximum RCC to [^{188}Re]ReO(N_2S_2-PEG_3-N_3) was increased to over 70% using 0.1 μg μL^{-1} of $SnCl_2$. At concentrations lower than this, more [^{188}Re]ReO_4^- was present, while higher concentrations resulted in more azide reduction to amine, thereby lowering the yield. Ensuring an inert atmosphere is therefore crucial to achieving the highest possible RCC in this labelling process.

Chelator concentration and reaction volume. The influence of the chelator quantity (0.01–0.5 μmol) and reaction volume (0.1–1.0 mL) on the RCC of [^{188}Re]ReO(N_2S_2-PEG_3-N_3) was determined (Fig. 6C and D). The activity (20 MBq), $SnCl_2$ concentration (0.1 μg μL^{-1}), temperature (90 °C) and time (60 min) were kept constant. The maximum RCC (~70%) was reached at a chelator quantity of 0.1 μmol, after which no further increase in conversion is observed. This equates to a relatively low apparent molar activity of 0.2 MBq $nmol^{-1}$, meaning that a post-labelling purification step is necessary. Lowering the amount of chelator in this labelling results in an increase in the percentage of [^{188}Re]ReO_4^- and [^{188}Re]Re(V)-citrate in the product mixture, thus reducing the overall yield. The maximal conversion of ~70% was also observed at the lowest reaction volume tested (0.1 mL), with an increase in the volume of citrate buffer leading to a steady decrease in RCC. This is as a result of the increase in the amount of [^{188}Re]ReO_4^- present in the final product mixture as the volume increased.

Reaction temperature and time. Finally, the reaction temperature (40 °C or 90 °C) and reaction time (15–60 min) were evaluated for the labelling of N_2S_2-PEG_3-N_3 (Fig. 6E). The activity

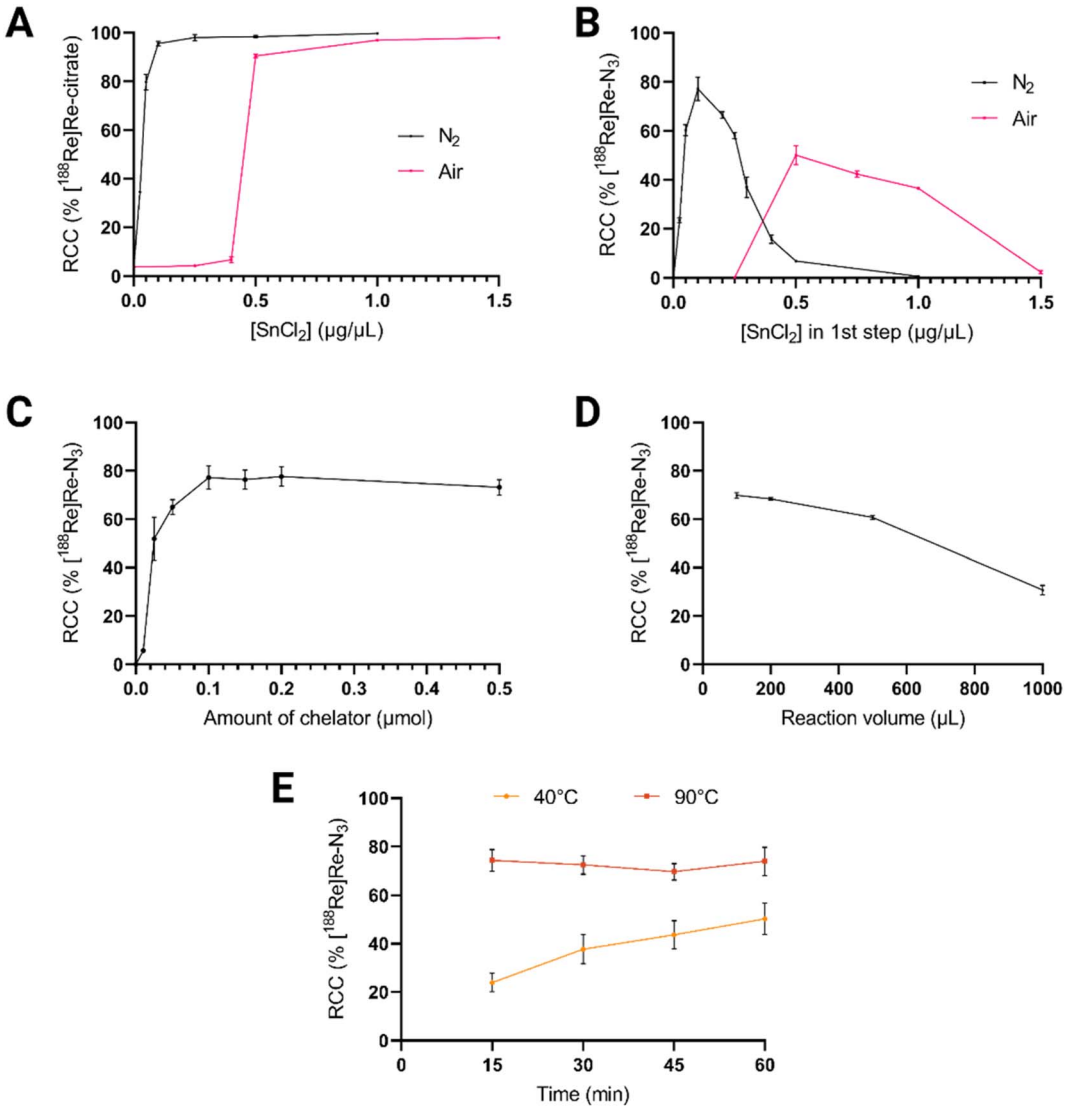

Fig. 6 Radiolabelling optimisation of [^{188}Re]ReO(N_2S_2-PEG_3-N_3). Conditions tested: (A) influence of N_2 atmosphere; (B) $SnCl_2$ concentration; (C) chelator quantity; (D) reaction volume; (E) reaction temperature and time. The fixed values for each variable during the optimisations were as follows: activity (20 MBq), $SnCl_2$ concentration (0.1 μg μL^{-1}), volume (100 μL), chelator quantity (0.1 μmol), temperature (90 °C) and time (60 min). RCC = radiochemical conversion.

(20 MBq), $SnCl_2$ concentration (0.1 μg μL^{-1}), volume (100 μL) and chelator quantity (0.1 μmol) were kept constant. At a temperature of 40 °C, the RCC was poor, only reaching ~50% after 1 h. At a temperature of 90 °C, however, the maximum RCC of ~70% was already reached after 15 min. These results confirm what is already known about the high temperatures required for producing ^{188}Re(v)-labelled compounds.[46]

The final reaction conditions for the transchelation from [^{188}Re]Re(v)-citrate (~140 MBq) to [^{188}Re]ReO(N_2S_2-PEG_3-N_3) are as follows: 0.1 μg μL^{-1} $SnCl_2 \cdot 2H_2O$ (from the first step), 0.1 μmol N_2S_2-PEG_3-N_3 (**4**), 100 μL total volume, 90 °C, 15 min. The pH of the reaction was kept around 5 using 1.0 M citrate buffer, as it has been shown that ^{188}Re(v)-radiolabelling is most efficient at a slightly acidic pH, likely because it prevents hydrolysis of the $SnCl_2$.[47,48] The final RCC of [^{188}Re]ReO(N_2S_2-PEG_3-N_3) was ~70%, which was then purified by prep-HPLC to yield a single peak in the radio-HPLC chromatogram (Fig. 7). Breakthrough of the unlabelled chelator during prep-purification was determined to be unlikely, as shown by the separation between the chelator and ^{nat}Re(v) complex, **Re-4**, when studied by HPLC (Fig. S36†). Additionally, the presence of a single peak and the fact that the reaction proceeds at a high temperature suggests there was complete conversion to the *syn* product with no *anti* diastereomer observed, a finding reported previously in literature.[45]

2.5 SPAAC click reaction

After purification of the labelled chelator, [^{188}Re]ReO(N_2S_2-PEG_3-N_3), and removal of the volatiles, the residue was redissolved in 25 μL of a 0.3 M sodium citrate solution (pH 8), which acted to neutralise any residual TFA and bring the final solution

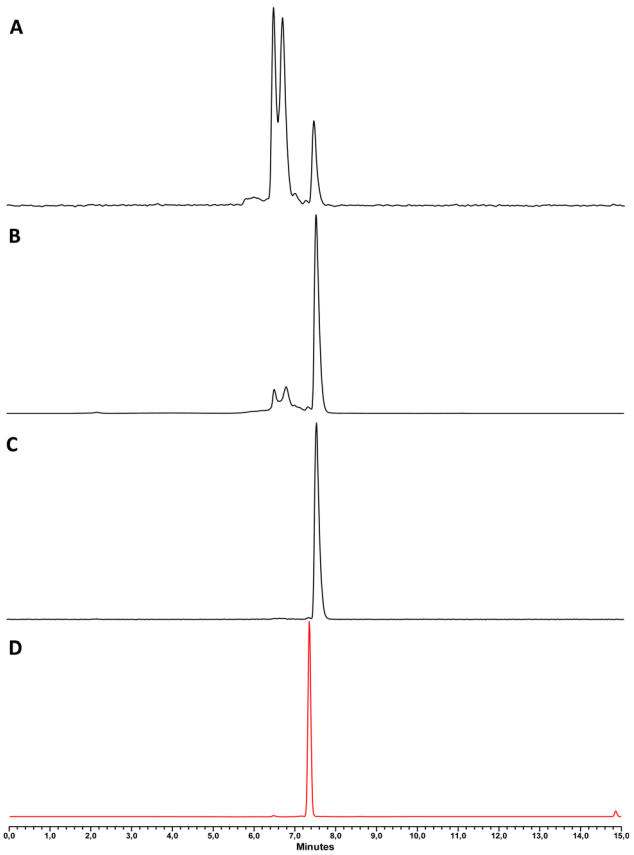

Fig. 7 Radio-HPLC chromatograms of (A) the unoptimised radiolabelling; (B) the optimised radiolabelling; (C) the final purified radiolabelling product, [^{188}Re]ReO(N_2S_2-PEG_3-N_3) and (D) UV chromatogram of ^{nat}ReO(N_2S_2-PEG_3-N_3) (358 nm).

to a pH of 5.5. To this solution, the DBCO-PEG_4-V_HH was added in HEPES buffer (enough to have an apparent molar activity of ~5 MBq nmol^{-1}), and the reaction was allowed to proceed for 30 min, after which time the extent of the click reaction was evaluated by iTLC (Fig. S37†). The yield of SPAAC click reaction ranged between 30-65%, resulting in a final apparent molar activity of between 1.4–3.3 MBq nmol^{-1}. Attempts at reaching a higher molar activity were not successful, likely due to the slower reaction kinetics of the SPAAC reaction. After 30 min, the [^{188}Re]Re-V_HH was purified from any non-V_HH-associated activity using a PD MiniTrap™ column, yielding the pure ^{188}Re-labelled V_HH-construct with a radiochemical purity (RCP) >99%. In an effort to try to improve the yield of the click reaction between the ^{188}Re-labelled N_2S_2 chelator and V_HH conjugate, the inverse electron demand Diels–Alder (IEDDA) reaction was adopted (Page S49 in the ESI†). Since the chelator bearing a tetrazine was also easily reduced in the presence of excess $SnCl_2$, this method was abandoned.

2.6 *In vitro* stability

When stored in saline without the addition of a quencher (*i.e.* ascorbate), the [^{188}Re]Re-V_HH radioconjugate exhibited a dramatic time-dependent decrease in radiochemical stability

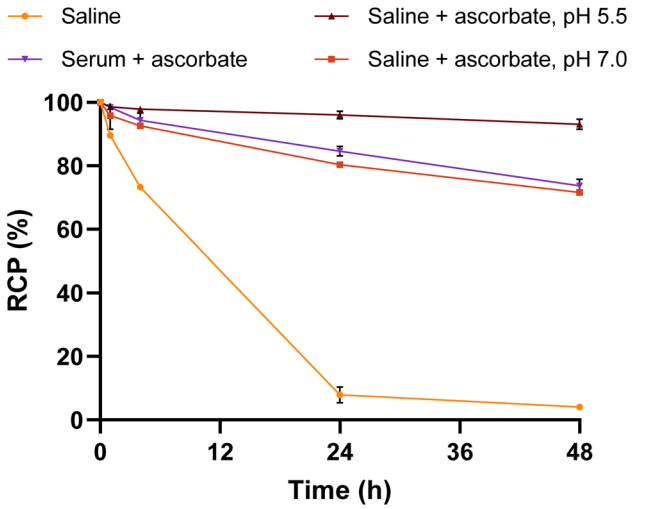

Fig. 8 *In vitro* stability of [^{188}Re]Re-V_HH in physiological saline (r.t.) or human serum (37 °C) over 48 h. Also included in the study is the influence of ascorbate and the pH of the solution. All solutions were monitored by iTLC and all saline solutions were also monitored by radio-HPLC over time. RCP = radiochemical purity.

due to the release of ^{188}Re from the complex, dropping to ~8% RCP after 24 h (Fig. 8). This was shown to be prevented by the addition of ascorbate at a slightly acidic pH of 5.5, whereby >96% of the conjugate was still intact after 24 h and >93% after 48 h. Radio-HPLC chromatograms of this solution show the decrease in RCP is as a result of the release of perrhenate from the conjugate over time without signs of V_HH or chelator degradation (Fig. S38†). Interestingly, the same concentration of ascorbate added at pH 7 did not keep the radioconjugate as stable as at pH 5.5, with the RCP gradually dropping to >80% and >71% after 24 h and 48 h, respectively. This indicates that having a slightly acidic environment aids in ensuring the stability of the [^{188}Re]Re(v)-N_2S_2 complex. Finally, upon incubation of the radioconjugate in human serum at 37 °C with the addition of ascorbate, the results mirrored those seen with the test in saline at pH 7. After 24 h, a moderate RCP of ~85% was observed.

2.7 *In vitro* cell-binding of [^{188}Re]Re-V_HH

To verify the c-Met binding affinity of the [^{188}Re]Re-V_HH construct, cell-binding experiments were performed with both a U87MG (glioblastoma) cell line and a BxPC3 (pancreatic cancer) cell line. Both cell lines are known to express c-Met.[49–51] Owing to our low molar activity, this experiment was performed with the cells in suspension to provide a greater surface area for binding compared to surface-adhered cells. After 2 h of incubation at 37 °C, only 3.17 ± 0.06% and 12.37 ± 0.19% of the radiolabelled V_HH was found to be associated with the U87MG and BxPC3 cells, respectively (Fig. 9). Receptor blocking studies to assess the specificity of the binding were performed by co-incubating cells with a 1000-fold excess of V_HH conjugated to *N*-ethylmaleimide (NEM). This decreased the binding by over 90% and 96% for the U87MG and BxPC3 cell lines respectively, proving the binding specificity of the V_HH.

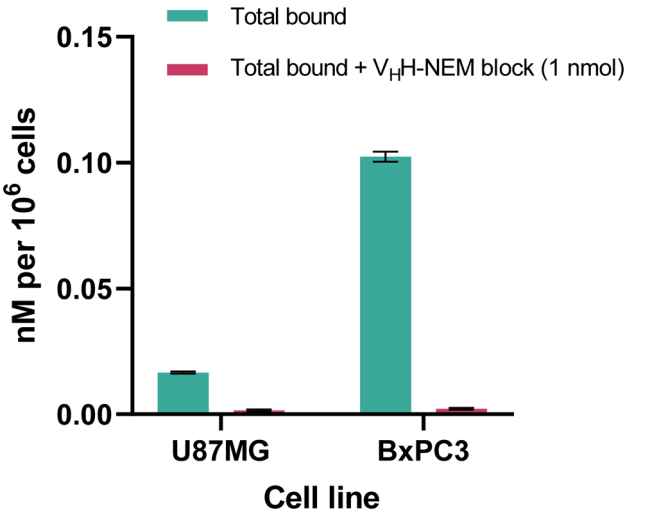

Fig. 9 *In vitro* cell-binding experiments with [^{188}Re]Re-V$_H$H against c-Met expressing U87MG and BxPC3 cell-lines. V$_H$H-NEM was used as a blocking agent.

2.8 *Ex vivo* biodistribution of [^{188}Re]Re-V$_H$H

Biodistribution studies were performed in order to evaluate the pharmacokinetic profile of the radioconjugate by injecting BxPC3 xenograft mice intravenously with [^{188}Re]Re-V$_H$H. Full biodistribution results are provided in the ESI.† Overall, low standardised uptake values (SUV) were calculated for all tissues of interest, including the blood, consistent with the rapid pharmacokinetics associated with V$_H$Hs (Fig. 10). Moderate excretion from the body was observed over time with 32.98 ± 6.06% of the injected activity being excreted after 4 h, climbing to 98.47 ± 0.22% after 48 h (Fig. S39†).[17] Fig. 10 shows that a high uptake was observed in the kidneys (SUV$_{4h}$ = 1.32 ± 0.24%) and liver (SUV$_{4h}$ = 1.12 ± 0.34%), which slowly washed out of these organs by 48 h p. i. (SUV$_{48h}$ = 0.26 ± 0.04% and 0.083 ± 0.02%, respectively). The higher kidney uptake was expected, as unbound V$_H$Hs are small enough to pass through the glomerular filter (~60 kDa) to be cleared from the bloodstream.[17,52] High uptake in the liver and intestines (Fig. S39†) indicate that there is some hepatobiliary clearance in addition to renal excretion. This could be a result of the lipophilicity of the chelator and SPAAC linker, as similarly high intestinal and liver uptakes were observed with a ^{186}Re-labelled N_2S_2 chelator[13] as well as a ^{99m}Tc-labelled HSA containing a SPAAC linker.[24] [^{188}Re]Re-V$_H$H exhibited minimal tumour uptake, which was at maximum at 4 h p. i. (SUV = 0.71 ± 0.27%) and slowly decreased over the subsequent timepoints. After 24 h p. i. however, only limited retention of the radioconjugate was observed in the tumour compared to other organs as the activity cleared from the bloodstream (tumour-to-blood ratio = 1.31 ± 0.51). Tumour-to-blood ratios for each timepoint can be found in Table S5.†

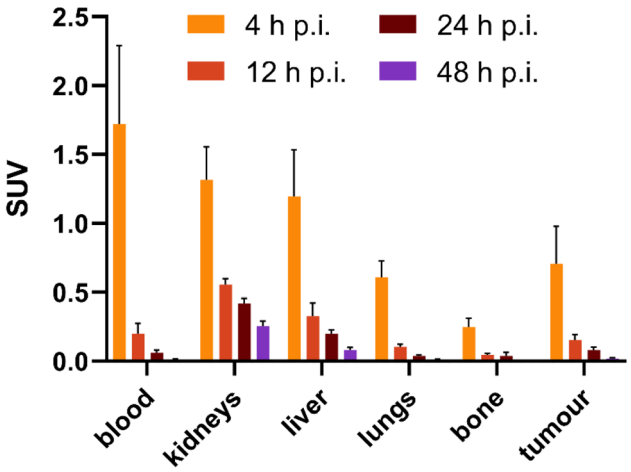

Fig. 10 *Ex vivo* biodistribution over time expressed as a standard uptake value (SUV) of [^{188}Re]Re-V$_H$H in male NMRI nude mice bearing BxPC3 tumour xenografts (n = 4). p. i. = post-injection.

3. Conclusion

In what we believe to be the first reported use of bioorthogonal click chemistry with ^{188}Re, we have successfully radiolabelled a HLE anti-c-Met V$_H$H with ^{188}Re(v) by employing a "chelate-then-click" approach. This was performed by designing and synthesising a bifunctional chelator in two halves which were joined post-labelling *via* SPAAC click chemistry. Cysteine-selective thiol-CA conjugation was achieved efficiently with the Michael-addition of the V$_H$H-SH monomer onto the DBCO-PEG$_4$-CA (**7**) half, resulting in the desired V$_H$H-DBCO construct. The radiolabelling of the N_2S_2-PEG$_3$-N$_3$ (**4**) chelator half, however, proved to be challenging as the excess $SnCl_2$ required to reduce the Re(VII) to Re(V) also reduced the azide on the chelator to an amine. Careful optimisation of the reactant quantities and conditions required for the labelling was performed, with the final optimised conditions resulting in a high RCC to [^{188}Re]ReO(N_2S_2-PEG$_3$-N$_3$) of ~70%. This was achieved by ensuring an inert atmosphere during the radiolabelling, thereby allowing the concentration of $SnCl_2$ used to be lowered dramatically. Reaction of the purified labelled chelator, [^{188}Re]ReO(N_2S_2-PEG$_3$-N$_3$), with the V$_H$H-DBCO conjugate resulted in the final SPAAC product, [^{188}Re]Re-V$_H$H, in high radiochemical purity and which displayed good *in vitro* stability over 48 h. Proof-of-concept studies for [^{188}Re]Re-V$_H$H as a c-Met targeting agent demonstrate specific binding *in vitro*, though suboptimal tumour uptake *in vivo*. Overall, this research displays the potential for the labelling of a biomolecule, such as a V$_H$H, with ^{188}Re by making use of the approach of bioorthogonal click chemistry.

Data availability

The data supporting this article has been included as part of the ESI.† Crystallographic data has been deposited at the CCDC under 2384422 and 2384423.

Author contributions

The research study was conceptualised by MO, GG and TO. Experimental design was carried out by DM, CS, MO and TO.

Production of ^{188}W for development of a ^{188}W/^{188}Re generator was done by MVdV. Generator fabrication, elution and analysis was performed by DM, MVdV and TO. Synthesis, bioconjugation, radiolabelling optimisation and stability studies were performed by DM and TO. X-ray crystal structure analysis was performed by OB. *In vitro* cell binding assays were performed by DM and CS. *Ex vivo* biodistribution experiments were performed by DM, CS, JW and MO. The first draft of the manuscript was written by DM, with all authors having contributed to manuscript review and editing, and having approved the final submission.

Conflicts of interest

The authors declare no competing financial interest.

Acknowledgements

The authors would like to acknowledge the contributions of Peter Casteels (Large Molecule Research Innovation, Sanofi, 9052 Ghent, Belgium) and Melissa Crabbé, Sunay Rodriguez Pérez, Koen Vermeulen and Amelie Coolkens (SCK CEN) to the research reported. We also thank Andrew Burgoyne for his help in initiating the project. The authors would also like to thank the SCK CEN Radioprotection Officers, Job Cools, Stefanie de Rudder, Zjef Beelen and Marc Eysermans, for their willingness to help with last-minute transports and to work late days for this project. This publication was partially created within the project SECURE funded by the European Union under grant agreement No. 101061230. The graphical abstract, Fig. 2, 4 and the graphical abstract were created with **http://BioRender.com**.

References

1 D. R. Melis, A. R. Burgoyne, M. Ooms and G. Gasser, *RSC Med. Chem.*, 2022, **13**, 217–245.
2 F. F. Knapp, *Int. J. Nuclear Med. Res.*, 2017, 3–15.
3 B. Ponsard, J. Hiltunen, P. Penttilla, H. Vera Ruiz, A. L. Beets, S. Mirzadeh and F. F. Knapp, *J. Radioanal. Nucl. Chem.*, 2003, **257**, 169–174.
4 U. Abram and R. Alberto, *J. Braz. Chem. Soc.*, 2006, **17**, 1486–1500.
5 P. S. Donnelly, *Dalton Trans.*, 2011, **40**, 999–1010.
6 A. Boschi, L. Uccelli, M. Pasquali, A. Duatti, A. Taibi, G. Pupillo and J. Esposito, *J. Chem.*, 2014, **2014**, 1–14.
7 S. S. Jurisson and J. D. Lydon, *Chem. Rev.*, 1999, **99**, 2205–2218.
8 J. R. Dilworth and S. I. Pascu, in *The Chemistry of Molecular Imaging*, Wiley, 2014, pp. 137–164.
9 M. Friebe, A. Mahmood, C. Bolzati, A. Drews, B. Johannsen, M. Eisenhut, D. Kraemer, A. Davison and A. G. Jones, *J. Med. Chem.*, 2001, **44**, 3132–3140.
10 M. Ono, R. Ikeoka, H. Watanabe, H. Kimura, T. Fuchigami, M. Haratake, H. Saji and M. Nakayama, *ACS Chem. Neurosci.*, 2010, **1**, 598–607.
11 K. Ogawa, T. Mukai, Y. Arano, H. Hanaoka, K. Hashimoto, H. Nishimura and H. Saji, *J. Labelled Compd. Radiopharm.*, 2004, **47**, 753–761.
12 T.-Y. Luo, I.-C. Tang, Y.-L. Wu, K.-L. Hsu, S.-W. Liu, H.-C. Kung, P.-S. Lai and W.-J. Lin, *Nucl. Med. Biol.*, 2009, **36**, 81–88.
13 D. W. Demoin, A. N. Dame, W. D. Minard, F. Gallazzi, G. L. Seickman, T. L. Rold, N. Bernskoetter, M. E. Fassbender, T. J. Hoffman, C. A. Deakyne and S. S. Jurisson, *Nucl. Med. Biol.*, 2016, **43**, 802–811.
14 M. D'Huyvetter, C. Xavier, V. Caveliers, T. Lahoutte, S. Muyldermans and N. Devoogdt, *Expert Opin. Drug Delivery*, 2014, **11**, 1939–1954.
15 M. Kijanka, B. Dorresteijn, S. Oliveira and P. M. van Bergen en Henegouwen, *Nanomedicine*, 2015, **10**, 161–174.
16 R. Chakravarty, S. Goel and W. Cai, *Theranostics*, 2014, **4**, 386–398.
17 P. Bannas, J. Hambach and F. Koch-Nolte, *Front. Immunol.*, 2017, **8**, 1603.
18 S. Hoefman, I. Ottevaere, J. Baumeister and M. Sargentini-Maier, *Antibodies*, 2015, **4**, 141–156.
19 V. Gupta, S. Bhavanasi, M. Quadir, K. Singh, G. Ghosh, K. Vasamreddy, A. Ghosh, T. J. Siahaan, S. Banerjee and S. K. Banerjee, *J. Cell Commun. Signaling*, 2019, **13**, 319–330.
20 G. Floresta and V. Abbate, *Med. Res. Rev.*, 2022, **42**, 1588–1606.
21 A. Sadiki, S. R. Vaidya, M. Abdollahi, G. Bhardwaj, M. E. Dolan, H. Turna, V. Arora, A. Sanjeev, T. D. Robinson, A. Koid, A. Amin and Z. S. Zhou, *Antibiot. Ther.*, 2020, **3**, 271–284.
22 D. Bauer, S. M. Sarrett, J. S. Lewis and B. M. Zeglis, *Nat. Protoc.*, 2023, **18**, 1659–1668.
23 D. Zeng, B. M. Zeglis, J. S. Lewis and C. J. Anderson, *J. Nucl. Med.*, 2013, **54**, 829–832.
24 N. A. Lodhi, J. Y. Park, K. Kim, Y. J. Kim, J. H. Shin, Y.-S. Lee, H.-J. Im, J. M. Jeong, M. Khalid, G. J. Cheon, D. S. Lee and K. W. Kang, *Mol. Pharm.*, 2019, **16**, 1586–1595.
25 V. Carroll, D. W. Demoin, T. J. Hoffman and S. S. Jurisson, *Radiochim. Acta*, 2012, **100**, 653–667.
26 L. Mei, Y. Wang and T. Chu, *Eur. J. Med. Chem.*, 2012, **58**, 50–63.
27 H. F. Kung, Y. Z. Guo, C. C. Yu, J. Billings, V. Subramanyam and J. C. Calabrese, *J. Med. Chem.*, 1989, **32**, 433–437.
28 C. S. John, L. C. Francesconi, H. F. Kung, S. Wehrli, G. Graczyk and P. Carroll, *Polyhedron*, 1992, **11**, 1145–1155.
29 R. A. Bell, B. E. McCarry and J. F. Valliant, *Inorg. Chem.*, 1998, **37**, 3517–3520.
30 L. G. Luyt, H. A. Jenkins and D. H. Hunter, *Bioconjugate Chem.*, 1999, **10**, 470–479.
31 B. Bernardim, P. M. S. D. Cal, M. J. Matos, B. L. Oliveira, N. Martínez-Sáez, I. S. Albuquerque, E. Perkins, F. Corzana, A. C. B. Burtoloso, G. Jiménez-Osés and G. J. L. Bernardes, *Nat. Commun.*, 2016, **7**, 13128.
32 B. Bernardim, M. J. Matos, X. Ferhati, I. Compañón, A. Guerreiro, P. Akkapeddi, A. C. B. Burtoloso, G. Jiménez-Osés, F. Corzana and G. J. L. Bernardes, *Nat. Protoc.*, 2019, **14**, 86–99.

33 A. D. Baldwin and K. L. Kiick, *Bioconjugate Chem.*, 2011, **22**, 1946–1953.
34 R. E. Nuttall, T. T. Pham, A. C. Chadwick, I. N. Hungnes, G. Firth, M. A. Heckenast, H. A. Sparkes, M. C. Galan, M. T. Ma and P. G. Pringle, *Inorg. Chem.*, 2023, **62**, 20582–20592.
35 T. T. Pham, I. N. Hungnes, C. Rivas, J. Cleaver, G. Firth, P. J. Blower, J. Sosabowski, G. J. R. Cook, L. Livieratos, J. D. Young, P. G. Pringle and M. T. Ma, *J. Nucl. Med.*, 2024, **65**, 1087–1094.
36 W. Shi, F. Tang, J. Ao, Q. Yu, J. Liu, Y. Tang, B. Jiang, X. Ren, H. Huang, W. Yang and W. Huang, *Angew. Chem.*, 2020, **132**, 20112–20116.
37 H.-Z. Zhu, G. Wang, H.-L. Wei, H.-J. Chu and J. Zhu, *Macromol. Res.*, 2016, **24**, 793–799.
38 J. O. Dickson, J. B. Harsh, W. W. Lukens and E. M. Pierce, *Chem. Geol.*, 2015, **395**, 138–143.
39 J. J. Vajo, D. A. Aikens, L. Ashley, D. E. Poeltl, R. A. Bailey, H. M. Clark and S. C. Bunce, *Inorg. Chem.*, 1981, **20**, 3328–3333.
40 J. Kleynhans, A. Duatti and C. Bolzati, *Molecules*, 2023, **28**, 1487.
41 S. Guhlke, A. Schaffland, P. O. Zamora, J. Sartor, D. Diekmann, H. Bender, F. F. Knapp and H.-J. Biersack, *Nucl. Med. Biol.*, 1998, **25**, 621–631.
42 J. L. Crudo, M. M. Edreira, E. R. Obenaus, M. Chinol, G. Paganelli and S. G. de Castiglia, *Int. J. Pharm.*, 2002, **248**, 173–182.
43 J. L. Crudo, M. M. Edreira, E. R. Obenaus and S. G. de Castiglia, *J. Radioanal. Nucl. Chem.*, 2004, **261**, 337–342.
44 G. Liu, S. Dou, J. He, D. Yin, S. Gupta, S. Zhang, Y. Wang, M. Rusckowski and D. J. Hnatowich, *Appl. Radiat. Isot.*, 2006, **64**, 971–978.
45 V. A. Sanders, D. Iskhakov, D. Abdel-Atti, M. Devany, M. C. Neary, K. R. Czerwinski and L. C. Francesconi, *Nucl. Med. Biol.*, 2019, **68–69**, 1–13.
46 Y. Feng, T. E. Phelps, V. Carroll, F. Gallazzi, G. Sieckman, T. J. Hoffman, C. L. Barnes, A. R. Ketring, H. M. Hennkens and S. S. Jurisson, *Dalton Trans.*, 2017, **46**, 14677–14690.
47 S. Prakash, M. J. Went and P. J. Blower, *Nucl. Med. Biol.*, 1996, **23**, 543–549.
48 L. Meléndez-Alafort, G. Ferro-Flores, C. Arteaga-Murphy, M. Pedraza-López, M. A. González-Zavala, J. I. Tendilla and L. García-Salinas, *Int. J. Pharm.*, 1999, **182**, 165–172.
49 H. Luo, H. Hong, M. R. Slater, S. A. Graves, S. Shi, Y. Yang, R. J. Nickles, F. Fan and W. Cai, *J. Nucl. Med.*, 2015, **56**, 758–763.
50 M. J. W. D. Vosjan, J. Vercammen, J. A. Kolkman, M. Stigter-van Walsum, H. Revets and G. A. M. S. van Dongen, *Mol. Cancer Ther.*, 2012, **11**, 1017–1025.
51 F. E. Escorcia, J. L. Houghton, D. Abdel-Atti, P. R. Pereira, A. Cho, N. T. Gutsche, K. E. Baidoo and J. S. Lewis, *Theranostics*, 2020, **10**, 151–165.
52 G. Bao, M. Tang, J. Zhao and X. Zhu, *EJNMMI Res.*, 2021, **11**, 6.